MODE II AND MIXED MODE I/II DELAMINATION OF GRAPHITE/EPOXY COMPOSITE UNDER DYNAMIC LOADING CONDITIONS

Sylvanus N. Nwosu[1], David Hui[2], and Gregory Czarnecki[3]

[1]*Department of Physics/Engineering, Dillard University, New Orleans LA 70122*
[2]*Department of Mechanical Engineering, University of New Orleans, LA 70122*
[3]*Wright Laboratory, Wright Patterson AF, Ohio 45433*

KEYWORDS: delamination, dynamic interlaminar fracture, pure mode, mixed mode, energy absorbed, split Hopkinson pressure bar

SUMMARY: This paper examines the split Hopkinson pressure application to mode II and mixed mode I/II delamination of unidirectional graphite/epoxy composites and the effects of dynamic loading on the energy release rate and absorption mechanism. The relationship between energy absorption and delamination follows a mode dependent power law behavior. Delamination increases linearly with mode ratio and impact energy depending on the mode of fracture. Maximum delamination is reached when the reflected wave is more than 15% higher than the incident wave. The results show regions of damage mechanisms. The dynamic energy released rate in the present model differs slightly from quasi-static model. The differences are attributed to scaling effect or strain rate sensitivity in dynamic mode fracture failure. However, the characteristics of modes I and II contributions to the energy release rate are the same as those observed in quasi-static test reported in the literature.

INTRODUCTION

Delamination is an interlaminar failure mode of fracture in laminated composite structures. In aerospace applications, there is always the danger of impact at high velocities which can cause a severe degradation of interlaminar and mechanical properties within a composite structure. Despite its importance, data for understanding the mode of failure and energy absorption mechanism of laminated composite plates under dynamic loading conditions are very limited. In laminated composites, the energy expended due to permanent plate damage is distributed among four different modes of fracture, namely, transverse matrix cracks, fiber fracture and fiber-matrix interface response and delamination with delamination identified as the dominant fracture mode in laminated graphite system [1]. Few reasons have been proposed for the course of delamination. In one case, delamination in a laminated plate was attributed to the formation of generator strip [2]. It was found that delamination begins when

a generator strip is formed and pushes on the adjacent ply. Earlier studies on the subject [3] found that the formation of the generator strip ceases when fibers within the layer are fully cut. Reflected tensile waves at interfaces and interlaminar shear waves are other mechanisms other than formation of generator strip that also contribute to delamination. Research by Tan et al. [4] suggested that vertical matrix cracks near laminate's top and bottom surfaces are due to bending stresses while slanted matrix cracks in the laminate are the result of transverse shear stress. Delamination was attributed to pure bending and shear induced crack propagation. In advanced laminated composites, Hui et al. [5] credited the impact generated delamination to the panel flexure due to the mode II type fracture in which shear forces play a dominant role, and also stated that delamination is possible when the amount of flexure reaches a critical value.

Generally, the resistance to failure can be characterized by interlaminar fracture toughness or energy release rate G. In their analysis of interlaminar fracture in uniaxial fiber-polymer composites based on beam theory analysis, Hashemi et al [6] developed a general equation based on bending moments applied to lower and upper sections of the plate. A general quasi-static expression for the energy release rate was given as

$$G = \frac{3}{4B^2h^3E_{11}}\left(\frac{M_1^{\,2}}{x^2} + \frac{M_2^{\,2}}{(1-x)^2} - (M_1 + M_2)^2\right) \tag{1}$$

$$G_I = \frac{6h_1^{\,3}}{B^2h_2^{\,3}(h_1^{\,3} + h_2^{\,3})E_{11}}\left(M_2 - \frac{h_2^{\,2}}{h_1^{\,2}}M_1\right)^2 \tag{2}$$

$$G_{II} = \frac{18h_1\ h_2}{B^2(h_1 + h_2)^2(h_1^{\,3} + h_2^{\,3})E_{11}}\left(M_2 + M_1\right)^2 \tag{3}$$

where h is half of the plate thickness, $x = h_1/2h$, and E_{11} is the axial modulus of the laminate, M_1 and M_2 are the moments of the lower and upper sections of the laminated plate about the crack tip, B is the total width of the plate, h_1 and h_2 are the thickness of the sections, respectively. Eqns. 2 and 3 also predict the presence of mode I in any loading condition in which h_1 is not equal to h_2. Reeder et al. [8] in their studies on failure criteria for mixed-mode delamination, introduced a closed form bilinear criteria based on changes in the failure mechanism of the delaminated surface. The energy release rate values were based on maximum load during the first load cycle, and included the effects of transverse shear deformation, rotation of the specimen at the delamination tip, and non-linear effects. Reeder et. al [9,10] had earlier noted the importance of including mixed-mode toughness testing when characterizing failure modes of a composite material. This is because laminated composite materials are often subjected to mixed-mode loading which results in a mixed-mode failure response that cannot be determined from pure mode toughness test following the standard procedure for interlaminar fracture toughness test developed by O'Brien et al. [11,12]. Thus, even in cases where pure mode II is certain to be the dominating mechanism, we maintain that a small fraction of mode I could be expected and should be evaluated. The G_I/G_{II} ratio from Eqns. 2 and 3 was approximated [13] as

$$\frac{G_I}{G_{II}} = \frac{4}{3}\left(\frac{3C - L}{C + L}\right)^2 \quad \textbf{(4)}$$

where C is the moment arm defined as perpendicular distance to the line of action of the loading force, $P_{c.}$ and L is the specimen span length. Eqn. 4 predicts a mixed ratio of 4/3 when $C = 0$ and $C = L$. For complete dynamic test analysis, kinetic energy, and rate effects must be considered for the total strain energy. Under dynamic loading conditions in which the crack is propagating at a certain speed, determination of stress intensity factors or energy release rates is very complex because the crack is mainly loaded by the stress wave. The mixed-mode interlaminar fracture toughness is therefore expected to depend mainly on the state of the stress around the crack front. Tensile pulse propagating through the material is mainly responsible for the crack propagation, and is reflected at the surface since the crack surface generally cannot transmit tension.

EXPERIMENTATION

The experimental set-up consists of (1) a stress generating system which comprised of a split Hopkinson bar and the striker, (2) special specimen fixture consisting of a specimen holder and indentor, (3) a stress measuring system made up of sensors (typically resistance strain gages), and (4) a data acquisition and analysis system. Each component of the system is described by Nwosu [14]. Dynamic loading of the composite plates was provided by a split Hopkinson pressure bar modified for perforation and fracture tests using appropriate specimen fixture and indentor.

Experimental parameters for AS4/3501-6 toughened epoxy composites used by Reeder et al. [8] are 131 GPa, 9.7 GPa, and 5.9 GPa for the longitudinal modulus (E_{11}), transverse modulus (E_{22}), and shear modulus (G_{12}), respectively. The dimensions of the graphite/epoxy specimens used in this present study are 52 mm in total span ($2L$), 25. 4 mm in width (B), and 0.27 mm/ply in thickness ($2h$). Dimensions were chosen to be of the same (2L/B) scale with Reeder et al.[8]. P_c, is the stress wave loading force, determined as the peak contact force in the force-displacement curve and is related to the stress field at the crack tip. This force is stress wave dependent, and is the driving force for the propagation of the stress field. Such stress has been shown not to be simply related to any externally applied force when the loading exceeded a certain value [8]. The delamination length, a, is determined by measuring the length of the mid-thickness crack along the specimen's edge. A microscope is used for clearer viewing of the extent of the delamination. When the specimen was pulled apart through the middle, it was observed that the length of the delamination zone measured from the edge to the crack tip was a little longer than the edge crack length due to the effects of deflection and curvature. In cases where the specimen is completely split through in mid-thickness by the loading force, the delamination length is taken as the total specimen span ($2L$).

Pure Mode II End Notch Flexure (ENF) Testing: The end notch flexure test is usually used for pure mode II test with the specimen loaded at the center, and simply supported near both ends. The ENF specimen for this investigation is shown in Fig. 1. The specimen is fabricated with 0.13 µm Teflon pre-crack placed at mid-thickness from one edge. Mode II fracture is expected to be

maximum when the loading is at the center because of the maximum bending effect. The energy released rate for this specimen is expressed as [6].

$$G_{II} = \frac{9}{16}\left(\frac{P_c^{\,2}(a + ch)^2}{B^2 h^3 E_{11}}\right) \qquad \textbf{(5)}$$

where c is a correction for some deflection, curvature effect, and rotation at the crack tip, and given as

$$c = \left[\frac{E_{11}}{11G_{12}}\left(3 - 2\left(\frac{\Gamma}{1+\Gamma}\right)^2\right)\right]^{1/2}$$
$$\Gamma = \frac{1..18\sqrt{E_{11}E_{22}}}{G_{12}} \qquad \textbf{(6)}$$

P_c is the critical load (the load at which the load-displacement curve deviates from a linear response) and delamination length, a, is determined by measuring the length of lamination or mid-thickness crack length. Moderate impact energy is needed to initiate the crack in the ENF specimen. At certain high strain rates, the crack propagates through the specimen, splitting it to the end.

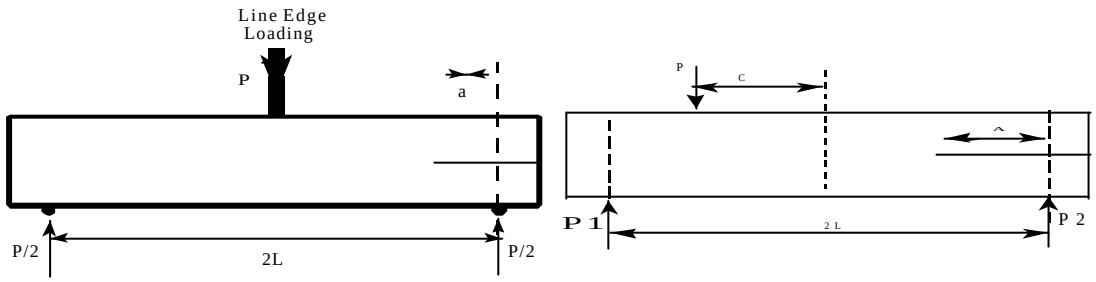

Fig. 1. Symmetrical (C = 0) loading for pure mode II end-notch flexure (ENF specimen) testing and (b) antisymmetrical (C > 0) loading for mixed-mode end-notch flexure testing (MENF specimen).

Center Notch Flexure Testing is same as in Fig. 1 for pure mode II fracture but with the a 0.13 um Teflon insert in the center mid-thickness located between the two middle plies. A line edge loading applied at the center creates a bending at the center with respect to the support at both sides of the specimen. Mode II is expected to dominate the fracture toughness with $C = 0$ since in-plane opening due to tension is negligible. Therefore $G_1 = 0$, and G_{II} is given by Eqn. 7 after replacing a in Eqn. 5 by $2a$.

$$G_{II} = \frac{9}{16}\left(\frac{P_c^{\,2}(2a + ch)^2}{B^2 h^3 E_{11}}\right) \qquad \textbf{(7)}$$

Mixed Mode Opening Notch Flexure (MONF): The configuration for the MONF specimen is shown in Fig. 2 in which the span of the upper half plane is longer than the lower plane and loaded by the reaction (P_I) at the support. The specimen was fabricated with 0.13 um Teflon pre-crack placed in

the mid-thickness from the opening edge. A line edge loading applied from the center simultaneously bends the specimen similar to ENF, and causes a reaction in the opposite direction at the opening section. Combination of the loading and the reaction pushes the specimen upper section open in tension creating an anti- symmetric mode I similar to an end-loaded specimen (ELS) while the flexure at the center, and reaction (P_{II}) contribute to shearing at the edges.

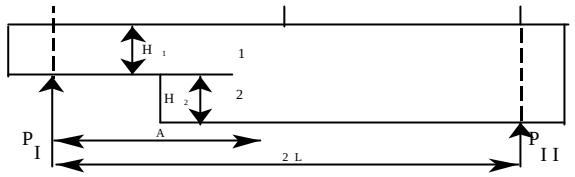

Fig. 2. Mixed I/II mode open-notch flexure test (MONF specimen)

Assuming equilibrium conditions, the forces (loading force and reaction at the supports) can be expressed as $P_I = P_C(L-C)/2L$ and $P_{II} = P_C(L+C)/2L$. Thus, MONF can be modeled as a mixed-mode ELS specimen proposed by William [7] with the components of the loading force replaced by the above expressions. Hence, the closed form model for MONF is expressed as

$$G_I^{\,m} = \frac{3}{4}\left(\frac{P_c^{\,2}(a+ch)^2(L-C)}{B^2h^3E_{11}\;L^2}\right)^2$$

$$G_{II}^{\,m} = \frac{9}{16}\left(\frac{P_c^{\,2}(a+ch)^2(L+C)}{B^2h^3E_{11}\;L^2}\right)^2 \qquad \textbf{(8)}$$

$$G_{TC} = G_I^{\,m} + G_{II}^{\,m}$$

where h = H in the figure. Note that Eqn. 8 reduces to ENF closed form (as it should) when $C = 0$ and predicts that MONF configuration gives 1/4 of the energy released rate given by ELS. This is expected because the conventional ELS specimen is fixed at one edge and loaded at the other edge. The current MONF configuration is freely supported such that the loading force is ½ the loading force in the ELS configuration. The mode ratio can be expressed as

$$\frac{G_I^{\,m}}{G_{II}^{\,m}} = \frac{4}{3}\left(\frac{L-C}{C+L}\right)^2 \qquad \textbf{(9)}$$

$$0 \le C < L$$

It is clear from the above closed form models that mode I is introduced when the loading is off-centered and increases as the specimen opens upward from the edge due to increased moment in the upper section of the plate. Eqn. 9 predicts a mixed ratio of 4/3 at $C = 0$ and 0 ($G_I = 0$) at $C = L$. This prediction agrees with the experimental results discussed below.

Mixed Mode End Notch Flexure testing (MENF specimen): Mixed-mode ratio could also be introduced in the ENF model by choosing an antisymmetrical (C > 0) loading. This is accomplished by varying the C value. Assuming equilibrium conditions for Fig. 2, and solving for the

forces (loading force and reaction at the supports), and moments about the crack initiation point C a closed form model for MENF is given as

$$G_I^{\ m} = \frac{3}{4}\left(\frac{P_c^{\ 2}(a+ch)^2 C^{\ 2}}{B^2 h^3 E_{11}\ L^2}\right)$$

$$G_{II}^{\ m} = \frac{9}{16}\left(\frac{P_c^{\ 2}(a+ch)^2}{B^2 h^3 E_{11}}\right) \qquad \textbf{(10)}$$

$$\frac{G_I^{\ m}}{G_{II}^{\ m}} = \frac{4C^2}{3L^2}$$

RESULTS AND DISCUSSION

Fig.3 shows variations of delamination with increasing impact energy for mixed-mode MONF cases. It is clearly evident in the figure that delamination once initiated increases as energy is increased. For the MONF specimen, about 1 J of impact energy was required to initiate interlaminar crack propagation, and 9.3 J for the crack to propagate the entire span ($2L$) of the specimen. Note that the delamination becomes constant and independent of impact energy after 9.3 J at G_I/G_{II} = 3/40, and 1/50 and 13 J for both G_I/G_{II} = 4/3 and G_I/G_{II} = 2/5. A plot of thickness normalized delamination in Fig. 5a clearly shows that the delamination is maximum at impact energy of 13 J. It was observed that energy above this value resulted in fragmentation and reduced delamination length of the specimen. For the ENF specimen (Fig. 3 b), the delamination was constant initially for impact energy below 20 J after which it increased gradually, reaching a maximum value after 74 J which corresponds to the splitting energy required for the crack to run the entire span. As in MONF, two to three regions of the failure mechanism are also evident. In the case of pure II CNF, no delamination was observed until a minimum energy of 26 J was reached after which the delamination remained constant [14]. As the impact energy is increased beyond 31 J, a drop in delamination with an increase in fragmentation is observed [14].

Fig. 4a shows that the delamination increases linearly the mode ratio. At low impact energy below 4 J, a 69% increase in impact energy results in only a 20% increase in delamination length. At a higher energy, a 56% increase in impact energy results in a 73% increase in delamination. This is mainly due to energy expended in the early stage to overcome friction and initiate the crack propagation. As more energy is pumped into the crack tip, delamination increases as the crack propagates. The result in Fig.4b indicates that a simple power law relationship exists between energy absorbed and delamination [14].

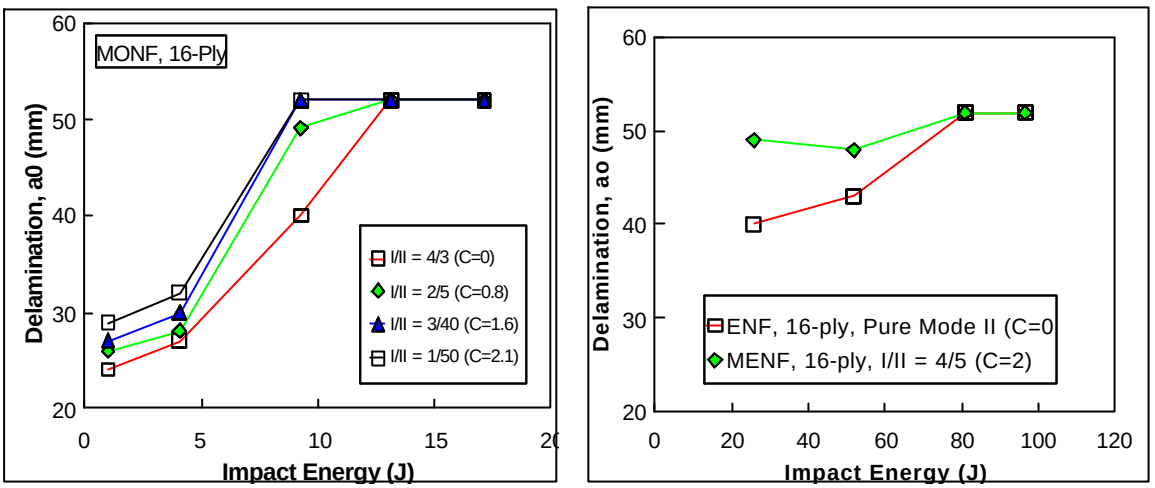

(a) (b)

Fig. 3. Effect of impact energy and mode ratio on delamination for (a) mixed mode and (b) mode II and asymmetric ENF loading.

Figs. 5 (a-b) display the variations of thickness normalized delamination length with impact energy and stress reflection coefficient. Delamination increases with impact energy and remains constant after 13 J in mixed mode (Fig.5a) and 74 J in ENF pure mode II (Fig. 5b). The reflection coefficient (the ratio of the amplitude of the reflected wave to amplitude of the incident wave) represents the fraction of the incident wave reflected at the indentor/specimen interface. The relative delamination increases sharply at 1.05 (Fig.5b) reaches a maximum at 25 (corresponding to maximum delamination without any fragmentation) when the coefficient is 1.15. The rate of crack growth increases sharply (as a results of internal damage matrix cracking) and begins to slow down as shown by the change in slope when the refection coefficient is 1.1 (i.e when the reflected wave is 10% higher than the incident wave) We conclude in general that the energy absorbed by the system increases with increase in the mode ratio or delamination.

The reflected wave is due to impedance mismatch and increases as the crack propagates through the interface to the surface. Thus, since it generally indicates surface damage, it is conceivable that increase in reflection coefficient in the region beyond 1.1 represents the region of surface crack, fiber breakage and delamination while below 1.10 represents internal matrix cracking. As expected, delamination remains constant for all impact energy greater than the impact energy required to split or fragment the specimen. This is equivalent to 13 J and 74 J (in Fig.3) in the cases of MONF and ENF configurations, respectively. Figs. 6 (a-d) compare the results of the present investigation with the closed form models presented by Reeder et al. [8]. The similarity of the results are reassuring that the loading configurations adopted here do simulate mixed-mode delamination comparable to the MMB test. The G_I / G_{II} results of the two models, however, differ slightly in values when $C > 0$ for the mixed mode tests.

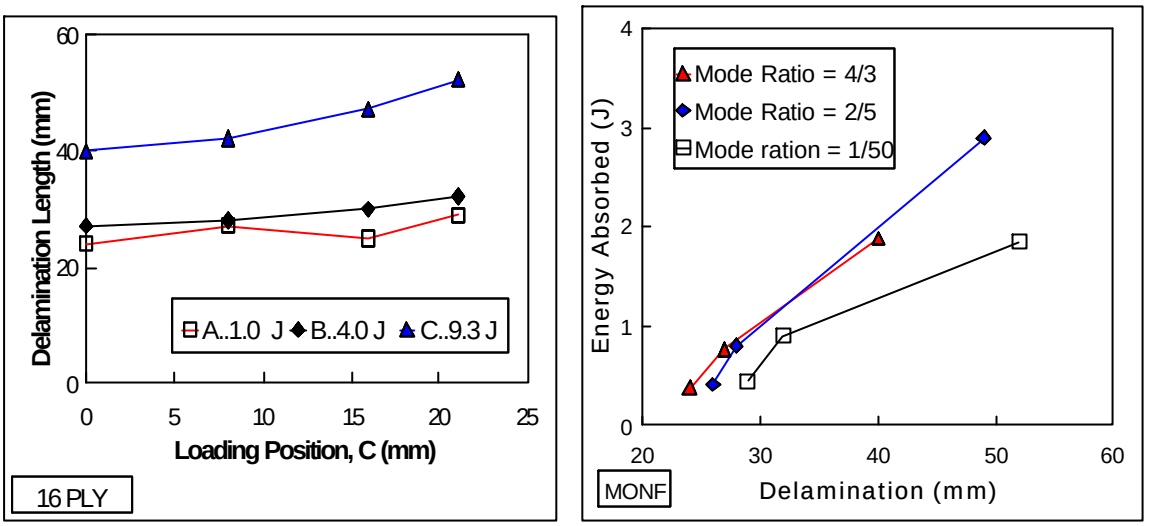

(a) (b)

Fig. 4. (a) Effect of mode ratio (loading position) and impact energy on delamination and (b) effect of mode ratio and delamination on energy absorption for mixed mode I/II.

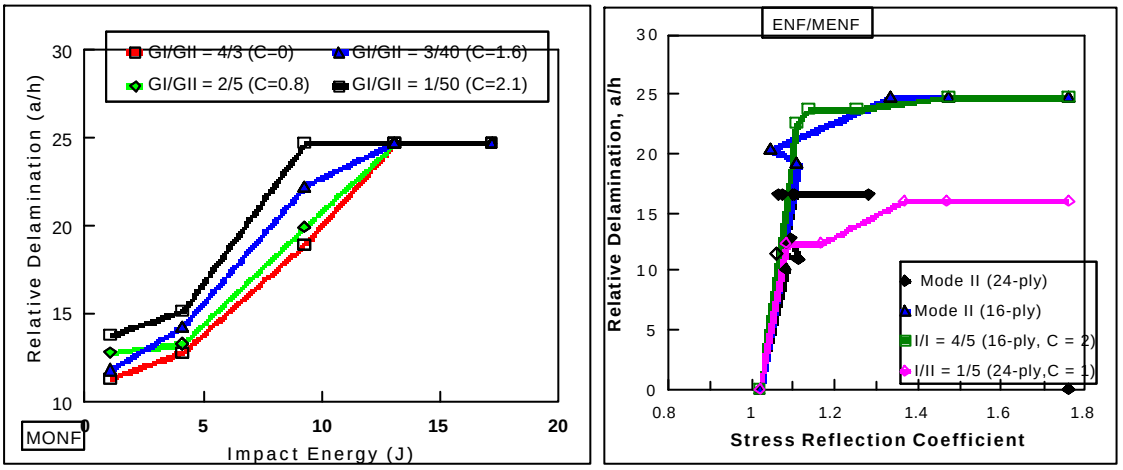

(a) (b)

Fig. 5. Variations of relative delamination length (a/h) with (a) impact energy (b) stress reflection coefficient (normalized reflected stress) for MONF and ENF/MENF specimens.

However, the mode ratio predictions of present model agrees with the experimental results better than the Reeder et al.[8] model that differ from experimental results by about 25%. This difference (Fig. 6d) could be attributed to strain rate sensitivity in the dynamic case compared to the quasi-static analysis [8]. Differences in the specimen dimensions are noted. Attempt was made to eliminate scaling effect by fabricating the specimen with same span/width (*2L/B*) ratio as in Reeder. et al [8]. It may be necessary to further normalize the two results in order to accurately quantify and characterize the difference or attribute it to strain rate effects.

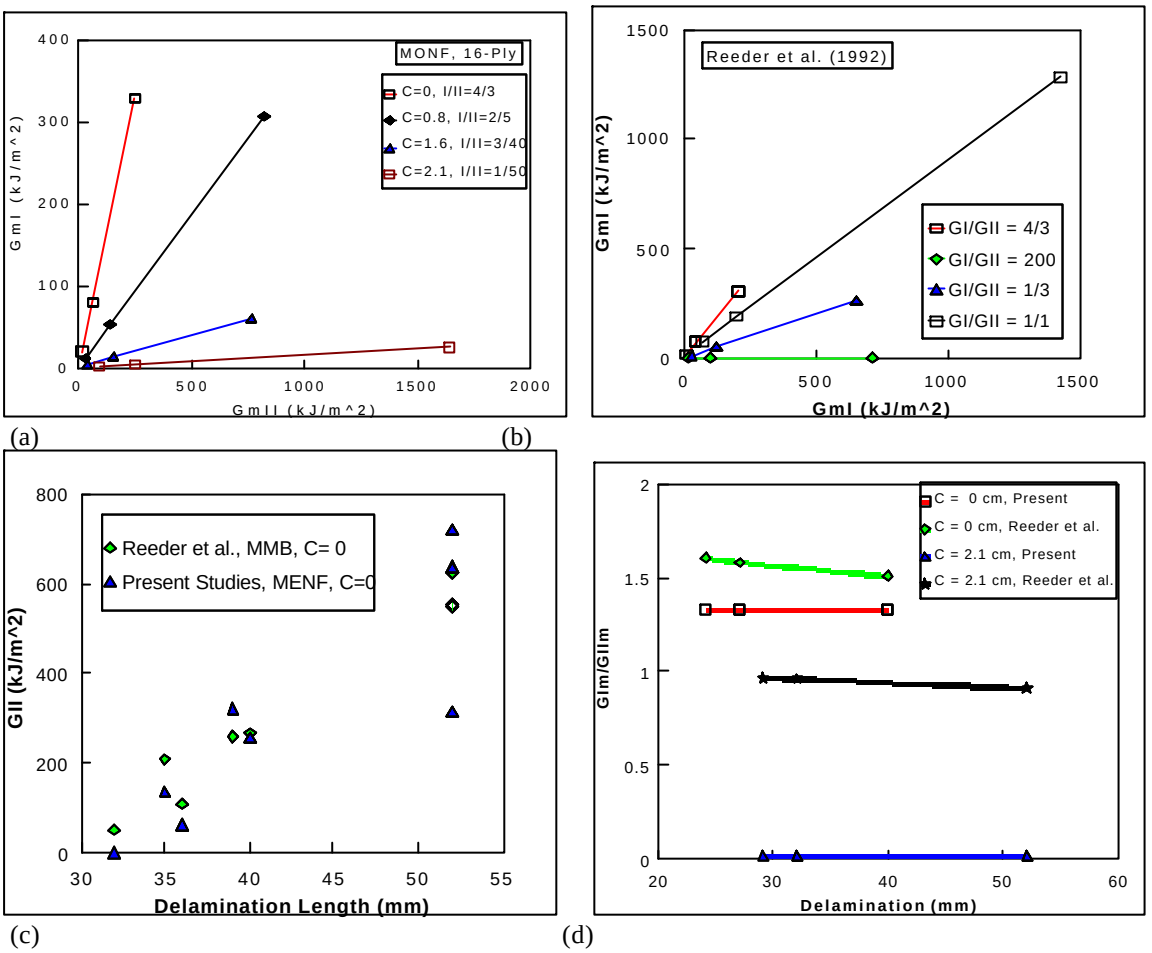

Fig. 6. Comparison of variation of G_I with G_{II} for mixed mode with delamination for the (a) present closed form MONF model, (b) MMB closed form model developed by Reeder et al. [8-9] effect of delamination on (c) G_{II} and (d) G_I/G_{II} ratio.

CONCLUSIONS

The relationship between energy absorbed and delamination follows a mode dependent power law behavior. Delamination increases with mode ratio and impact energy up to a certain maximum depending on mode of fracture, with CNF >ENF>MONF. Maximum constant delamination (specimen span) is reached when the reflected wave is more than 15% higher that the incident wave. Matrix crack, fracturing, and crack propagation (leading to splitting) are seen as three distinct failure regions for graphite/epoxy. The dynamic energy released rate according to the present model exhibits some similarities in pure mode II test with the quasi-static cases reported by Reeder et al. [8]. Mode I and Mode II contributions to the total fracture toughness seem to be the same in the two models. Some differences exit between the two models in the prediction of mixed mode failure and were attributed to strain sensitivity in the dynamic case presented here. More energy is absorbed in pure mode II than in mixed mode I/II.

ACKNOWLEDGMENT

This work was supported by Flight Dynamics Directorate, Wright Laboratory, Wright Patterson Air Force Base under contract N0. F33615-93-C3411, Dillard University, New Orleans, LA and Conrad N. Hilton Endowment for Physics.

REFERENCES

[1]. Zukas, J. A., Nicholas, T., Swift, H. F., Greszczuk, L. B., and Curran, D. R... *Impact Dynamics* ,Krieger Publishing Co., Florida, 1992

[2]. Sierakowski, R. L., Ross, C. A., and Malvern, L. E., "Studies on the Fracture Mechanisms in Partially Penetrated Filament Reinforced Laminated Plates", *U. S. Army Research Office, DAAG 29-79-G-0007, December 1982.*

[3]. Cristescu, N., L. E. Malvern, R. L. Sierakowski, "Failure Mechanism in Composite Plates Impacted by Blunt-Ended Penetrators, Foreign Object Damage to Composite", *ASTM STP* 568, 1975, pp 27-172.

[4]. Tan, T.M and Sun, C.T., "Wave Propagation in Graphite/Epoxy Laminates Due to Impact," *J. Appl. Mech.*, Vol. 52, pp. 6-12 , 1985.

[5]. Hui, D.,"Theoretical Modeling of the Perforation of Laminated Plates by Rigid Projectiles", final report, 1990 *AFOSR Summer Faculty Research Program*, September 1990.

[6]. Hashemi, S, Kinlogh A,K, and Williams, JG (1990), "The analysis of Interlaminar Fracture in Uniaxial Fiber-polymer composites," *Proc. of Royal Society, London*, A427, 173-199

[7]. Williams, G, " On the Calculation of Energy Release Rate for Cracked Laminates," *International Journal of Fracture*, Vol. 36, 1988, pp. 101-119.

[8]. Reeder, James (1993), "Bilinear Failure Criterion for Mixed Mode Delamination,"*Composite Materials: Testing and Design* Vol. 11, ASTM STP 1206, Am. S. for testing and Materials, Philadelphia, p 303-322

[9]. Reeder, J. R. and Crews, J.H,Jr (1990), " Mixed mode bending Method for Delamination Testing," *AIAA Journal*, Vol. 28, No. 7, 1990, p. 1270.

[10]. Reeder, J. R. and Crews, J.H,Jr (1992), " Redesign of Mixed Mode Bending Test to Reduce Nonlinear Effects," *JCTRER*, Vol. 14, No. 1, Spring 1992. p. 12-19.

[11]. O'Brien, T. K. and Martin, R. H., Round Robin Testing for Mode I Interlaminar Fracture Toughness of Composite Materials," *J. Composite Technology and Research*, JCTER, Vol. 15, No. 4, Winter 1993,pp. 269-281

[12] Standard Test Method for Mode I Mode I Interlaminar Fracture Toughness of Unidirectional Fiber-Reinforced Polymer Matrix Composites in ASTM Annual Book of Standards, Vol, 15.03, pp. 272-280. O'Brien, KT and Martin, RH

[13]. Sriram, P., Khourchid, Y, Hooper, S.J, and Martin, R.H., "Experimental Development of Mixed-Mode Fatigue Delamination Criterion," *Composite Materials: Testing and Design* Vol. 5, ASTM STP 1230, Am. S. for testing and Materials, Philadelphia, 1995, p 3-18

[14]. Nwosu, S.N, " High Strain Rate Perforation and Mixed Mode Delamination of Laminated Composite, *Wright Laboratory, Report # WL-TR-3080*, 1997.